I. OUTLINE OF GH77-1 CRUISE AND ITS RESULTS

Tomoyuki Moritani

Introduction

This report of the GH77–1 cruise includes mainly the results of the on-board surveys and observations in the survey area of the medial-western part of Central Pacific Basin (6°–11°N, 175°30′–179°W), and partly the results of the on-shore analytical works on the obtained samples. In addition, some results of the geophysical works along the tracks from off Japan through southwest of Kwajalein and Majuro of Marshall Islands to the survey area are described in Appendixes I–III (Fig. I–1).

The GH77–1 cruise of the R/V Hakurei-maru (1,821.6 T) was carried out from the 12th of January to the 12th of March, 1977, as the third phase field work of the GSJ* five year research program of "Study on the manganese nodule deposits of the Central Pacific Basin" and also as a part of NRIPR** research program of "Technological study on the exploitation of deep sea mineral resources".

The GSJ research program (F.Y. 1974–F.Y. 1978) aims at providing information on the manganese nodule distribution and their origin on the deep sea floor of the Central Pacific Basin bounded by the Marshall Ridge to the west, the Christmas Ridge to the east, and the Mid-Pacific Mountains to the north.

The first phase of the investigation was carried out during the GH74–5 cruise in the eastern part of the Basin (6°–10°30′N, 164°30′–171°30′W) (Mizuno and Chujo *eds.*, 1975), the second phase was done during the GH76–1 cruise in the central-eastern part (5°–10°N, 170°–175°W) (Mizuno and Moritani *eds.*, 1977), and the present third phase covered an area of about 5° square, in the central-western part of the Basin, just west of the GH76–1 area (Fig. I–2).

Outline of GH77–1 cruise

Participants of the present cruise were twelve scientists from GSJ, NRIPR, and MMAJ***, seven graduate and undergraduate students as technical assistants from two universities, and one trainee scientist from Apia Observatory under UN fellowship (Table I–1).

The R/V Hakurei-maru commanded by Captain H. Okumura sailed from Funabashi Port, Tokyo Bay on 12th of January, 1977, made various surveys and observations in the survey area of the Central Pacific, called Majuro Port, Marshall Islands for 3 days and Apia Port, West Samoa for 5 days on the way, and returned to Funabashi on the 12th of March of the same year.

The roughly summarized program and the detailed daily program of sixty days of the

*GSJ stands for Geological Survey of Japan.

**NRIPR stands for National Research Institute for Pollution and Resources.

***MMAJ stands for Metal Mining Agency of Japan.

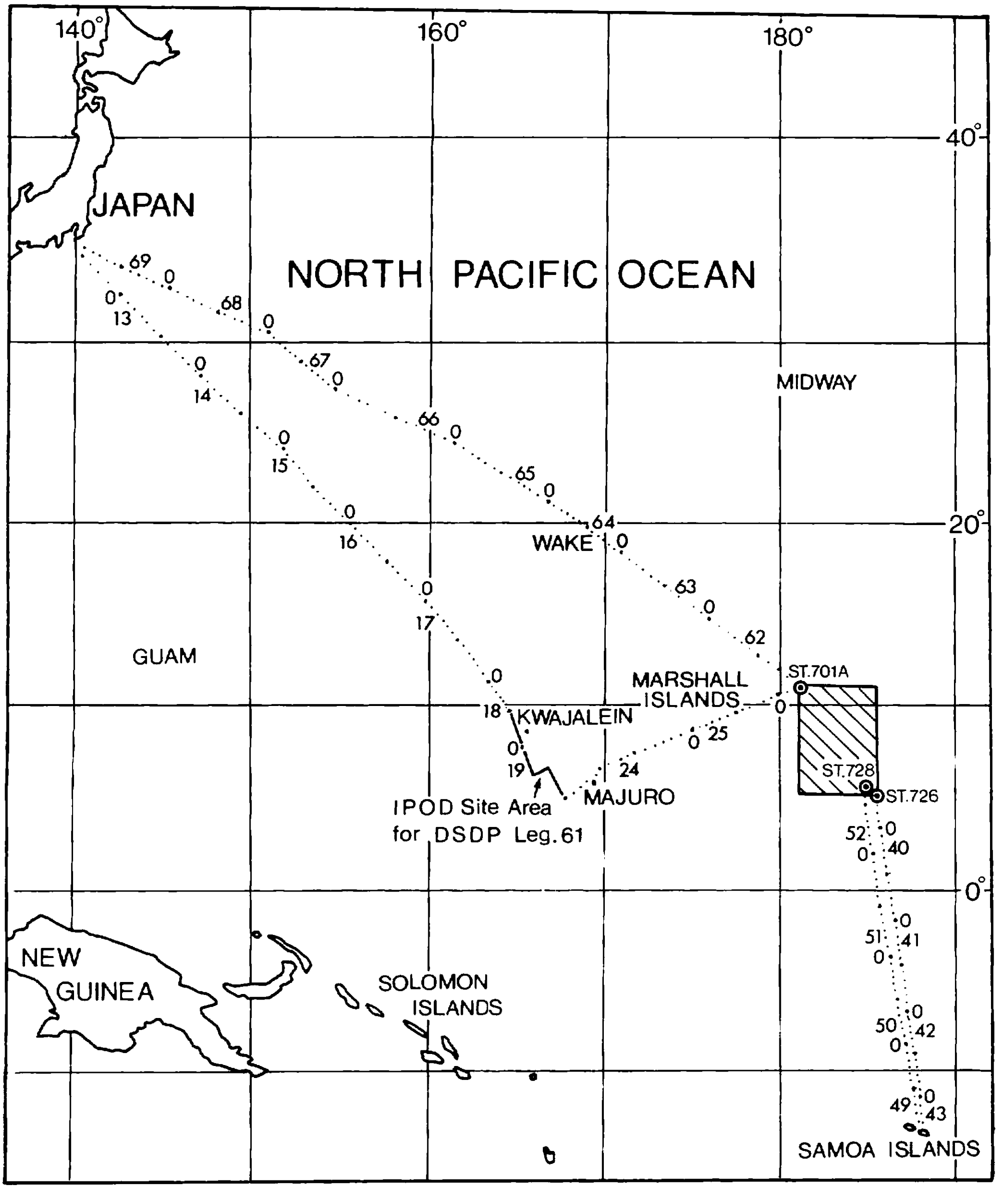

Fig. I–1 Index map of the survey areas and tracks.

cruise are shown in Tables I–2 and I–3 respectively.

Of the total sailing distance of 18,565 km (12,213.8 n.m.), 6,919 km (3,736 n.m.) was spent for geological, optical, and geophysical observations in the survey area during twenty-four days. Along the tracks between Japan and the survey area, one via westward of Kwajalein and Majuro, Marshall Islands, and the other directly, and between the survey area and Apia, West Samoa, a geophysical survey was continuously carried out by means of 12 kHz PDR and 3.5 kHz PDR, and proton magnetometer, and on-board

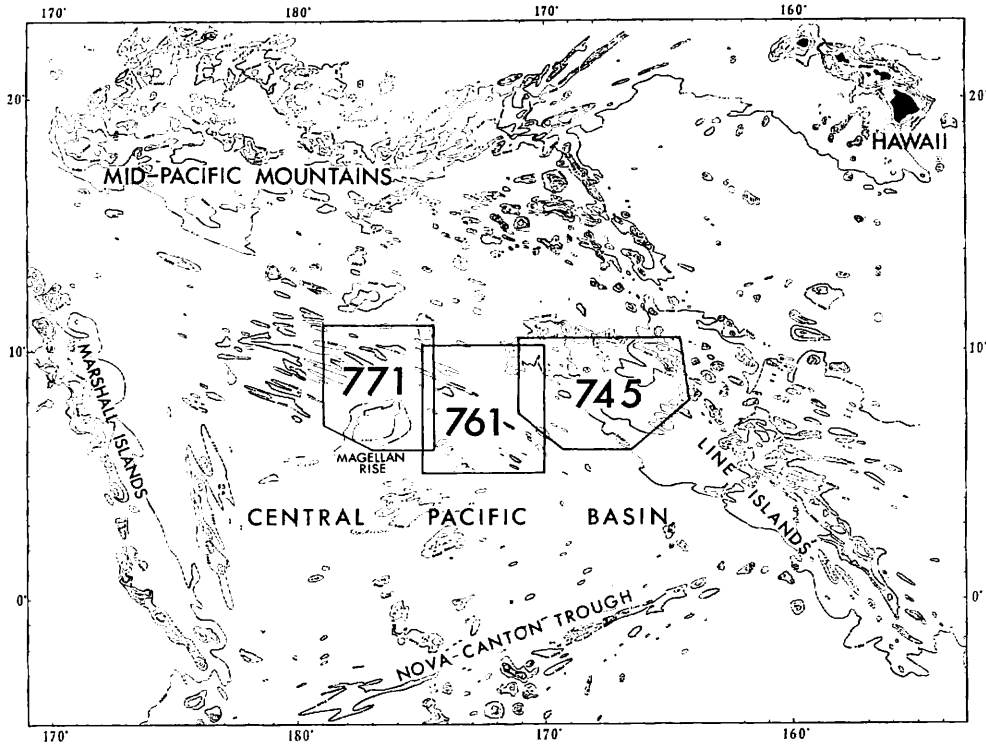

Fig. I–2 Submarine topography and survey areas of GH77–1, GH76–1, and GH74–5 cruises in the Central Pacific Basin. Data source of topographic map: WINTERER, EWING *et al.* (1973).

gravity meter.

During the course from Japan to the survey area, along the scheduled IPOD site area for DSDP Leg 61, southwest of Kwajalein, a continuous seismic reflection profiling was carried out together with other geophysical surveys to get some geophysical reference information for the project.

Survey methods at the GH77–1 area

The survey methods used in the survey area are shown in Table I–4. These include sailing surveys of various geophysical methods, stationary or on-site observations such as geological sampling, sea bottom photographing and STD measurement, and on-board observations and analyses of obtained sediments and manganese nodules.

Fundamental stations were arranged firstly in grids of about 110 km (1° in latitude and longitude) and covered in earlier half survey of the cruise, and then secondly some additional stations were set in the later half of the cruise in the middle points between the fundamental ones, especially so as to delineate the distribution of the high nodule abundance, in the northeastern or eastern parts of the survey area (Fig. I–3—6).

At each fundamental station, sampling by an Okean(Ocean)-70 grab and associated simultaneous sampling and photographing of the bottom by two sets of freefall (boom-

Table I–1 On-board scientific staffs.

Name	Organization	Speciality and responsibility
Tomoyuki MORITANI	G.S.J.	Chief scientist; geology and mineralogy.
Shuji MARUYAMA	G.S.J.	Co-chief scientist; feasibility study of ore deposit and technical aspects on on-site observation.
Seizo NAKAO	G.S.J.	Senior scientist; geology and sedimentology.
Koji ONODERA	G.S.J.	Scientist; topography.
Yasumasa KINOSHITA	G.S.J.	Scientist; geology and sedimentology in relation to optical survey.
Masato NOHARA	G.S.J.	Scientist; mineralogy and geochemistry.
Masato JOSHIMA	G.S.J.	Scientist; geophysics (magnetic and gravimetric survey) and NNSS positioning.
Fumitoshi MURAKAMI	G.S.J.	Scientist; geophysics (magnetic and continuous seismic reflection survey).
Norio YAMAKADO	N.R.I.P.R.	Senior scientist; exploitation techniques of nodules and engineering property of sediments.
Keiji HANDA	N.R.I.P.R.	Scientist; exploitation techniques of nodules and engineering property of sediments.
Toshio KOIZUMI*	M.M.A.J.	Scientist; survey techniques.
Tadashi ITO**	M.M.A.J.	Scientist; survey techniques.
Akira USUI	Univ. of Tokyo	Graduate student; technical assistant.
Takafumi NISHIOKA	Kobe Univ.	Undergraduate student; technical assistant.
Hiroyuki MIKI	Kobe Univ.	*Ibid.*
Masayuki HYODO	Kobe Univ.	*Ibid.*
Ikuo KATSURA	Kobe Univ.	*Ibid.*
Kazutaka TAKAHASHI	Kobe Univ.	*Ibid.*
Masahiko YOKOTA	Kobe Univ.	*Ibid.*
Frank F. WINTERSTEIN**	Apia Observatory	Scientist; trainee on marine geological survey.

*On-board from Funabashi to Apia.
**On-board from Apia to Funabashi.

erang) photo grabs were regularly carried out. This aimed at providing the data for checking the horizontal distribution of surficial sediments and nodules over a very limited one station area. Then, at the additional stations, besides the usual samplings, five core samplings, two sea bottom photographings, and two samplings of large amount of nodules by larger box dredge were made.

Also, water measurement by STD graphic recorder was carried out along 178°W meridian (St. 706—St. 710), concurrently with Okean-70 grab sampling. However, the deep sea TV was not tried because of the worse sea condition during all the time in the survey area.

The geophysical survey tracks were arranged to connect each neighboring station, mainly in north-south direction so as to cut the general trend of topographic relief and magnetic anomaly trend (WINTERER, EWING *et al.*, 1973; LARSON *et al.*, 1972). These geophysical surveys by means of 12 kHz and 3.5 kHz PDRs, continuous seismic reflec-

Table I–2 Rough summary of cruise program.

Jan. 12*	Lv.	Funabashi (14: 15). Geophysical survey from off Boso Peninsula via Kwajalein to Majuro.
Jan. 21	Ar.	Majuro (13: 30).
Jan. 24	Lv.	Majuro (17: 00). Geophysical survey from Majuro to the survey area.
Jan. 26	Ar.	the survey area. Geological and geophysical survey.
Feb. 9(8)	Lv.	the survey area. Geophysical survey from the survey area to Apia.
Feb. 13(12)	Ar.	Apia (09: 00).
Feb. 18(17)	Lv.	Apia (16: 00). Geophysical survey from Apia to the survey area.
Feb. 22(21)	Ar.	the survey area. Geological and geophysical survey.
March 3(2)	Lv.	the survey area. Geophysical survey from the survey area to off Boso Peninsula.
March 12	Ar.	Funabashi (08: 00).

*Shown both in Japan date and on-site date (in the parentheses).

Table I–4 Observation methods at the survey area.
The right-hand column shows a survey line length and an observation number of respective work.

Cruising and positioning by NNSS	ca. 6,919 km (3,736 n.m.)
Geophysical methods	
Bathymetric survey by 12 kHz PDR	ca. 6,623 km (3,576 n.m.)
Subbottom profiling by 3.5 kHz PDR	ca. 6,623 km (3,576 n.m.)
Continuous seismic reflection profiling by air-gun	ca. 6,012 km (3,246 n.m.)
Magnetic survey by proton magnetometer	ca. 6,623 km (3,576 n.m.)
Gravimetric survey by on-board gravimeter	ca. 6,919 km (3,736 n.m.)
Geological methods	
Bottom sampling by Okean (Ocean)-70 grab	G372–405
Bottom sampling by large box dredge	D211–212
Bottom sampling by freefall (photo) grab	FG33–72
Bottom sampling by piston corer	P97–101
Optical methods	
Observation by deep sea still camera	C11–12
Observation by freefall photo grab one-shot camera	FG33C–72C
Others	
Water measurement by STD	S6–10
On-board examinations on sediments and nodule samples	
Compositional analysis of sediment; soft X-ray photography of sediment; sampling of interstitial water in the sediments by low-pressure squeezer; size and type classification of nodules; X-ray diffractometer analysis of nodules; X-ray fluorescence analysis of nodules.	

Table 1–3 Daily program of cruise.

Date*	Weather**	Cruising time	Cruising distance***	Remarks****
Jan. 12	bc, o, b	09.45	130.9	Lv. Funabashi (14: 15).
13	o, r, bc, d	23.30	346.8	(Geophysical survey) from off Boso Peninsula.
14	o, r, c	23.30	341.8	(Geophysical survey).
15	o, c, bc, d	23.30	341.3	(Geophysical survey); test of fixed wire of proton magnetometer.
16	bc, c, d, o	23.30	333.5	(Geophysical survey).
17	bc, b	23.30	328.6	(Geophysical survey).
18	bc, b	23.30	301.0	Geophysical survey in the scheduled IPOD site area for DSDP Leg 61, southwest of Kwajalein.
19	bc, b	24.00	251.9	Geophysical survey in the same above area.
20	bc, b, c	24.00	276.4	Geophysical survey in the same above area, and (geophysical survey) from there towards Majuro.
21	b, c, o	12.00	127.6	(Geophysical survey); ar. Majuro (13: 30); open house.
22	bc, b	—	—	—
23	c, o, q	—	—	—
24	c, bc, o	07.00	95.5	Lv. Majuro (17: 00); (Geophysical survey).
25	bc	24.00	325.7	(Geophysical survey).
26	bc, c	24.00	251.7	(Geophysical survey); ar. the survey area; geophysical survey and sampling (St. 701); (passed the 180° meridian).
27 (26)	bc, c, o	24.00	150.0	Geophysical survey and sampling (Sts. 702 and 703).
28 (27)	bc, o	24.00	159.9	Geophysical survey and sampling (Sts. 704 and 705).
29 (28)	bc, o, b, c	24.00	160.9	Geophysical survey and sampling (Sts. 706 and 707).
30 (29)	bc, b, c	24.00	155.9	Geophysical survey and sampling (Sts. 708 and 709).
31 (30)	bc	24.00	159.6	Geophysical survey and sampling (Sts. 710 and 711).
Feb. 1 (31)	bc, c	24.00	161.3	Geophysical survey and sampling (Sts. 712 and 713).
2 (Feb. 1)	bc	24.00	172.9	Geophysical survey and sampling (Sts. 714 and 717).
3 (2)	bc, b, c	24.00	164.8	Geophysical survey and sampling (Sts. 718 and 719).
4 (3)	bc	24.00	191.3	Geophysical survey and sampling (Sts. 720 and 721).
5 (4)	bc, b, o	24.00	180.7	Geophysical survey and sampling (Sts. 722 and 723).
6 (5)	bc, b	24.00	143.8	Geophysical survey and sampling (Sts. 724 and 725).
7 (6)	c, o, bc, q	24.00	179.2	Geophysical survey and sampling (Sts. 716 and 715).
8 (7)	o, r, d, b	24.00	162.8	Geophysical survey and sampling (Sts. 727 and 726).
9 (8)	o, bc, c	23.30	263.0	Geophysical survey; lv. the survey area; (Geophysical survey).
10 (9)	bc, b	23.30	303.9	(Geophysical survey).
11 (10)	bc, c	24.00	327.4	(Geophysical survey).

12 (11)	bc, b	24.00	195.4	(Geophysical survey).
13 (12)	bc, b	09.00	84.0	(Geophysical survey); ar. Apia (09: 00).
14 (13)	b	—	—	—
15 (14)	b, bc	—	—	—
16 (15)	bc, c	—	—	—
17 (16)	bc, b	—	—	—
18 (17)	bc	08.00	106.8	Lv. Apia (16: 00); (Geophysical survey).
19 (18)	bc, c	24.30	341.8	(Geophysical survey).
20 (19)	bc, b	24.30	346.9	(Geophysical survey).
21 (20)	bc, c	24.00	330.7	(Geophysical survey).
22 (21)	c, bc, b, o	24.00	221.5	(Geophysical survey); ar. the survey area; geophysical survey and sampling (St. 728).
23 (22)	bc, b	24.00	163.5	Geophysical survey and sampling (Sts. 729 and 730).
24 (23)	bc	24.00	153.0	Geophysical survey and sampling (Sts. 731 and 732).
25 (24)	bc, c, o	24.00	141.0	Geophysical survey and sampling (Sts. 733 and 733A).
26 (25)	bc, b	24.00	144.4	Geophysical survey, sampling (Sts. 734 and 735), and optical survey (St. 735).
27 (26)	c, bc	24.00	141.8	Geophysical survey and sampling (Sts. 722A and 736).
28 (27)	c, bc	24.00	137.5	Geophysical survey, sampling (Sts. 737 and 738), and optical survey (St. 737).
March 1 (28)	bc, c	24.00	192.5	Geophysical survey and sampling (Sts. 719A and 739).
2 (1)	bc, b	24.00	221.0	Geophysical survey and sampling (St. 703A).
3 (2)	bc, b	24.00	270.9	Geophysical survey and sampling (St. 701A); lv. the survey area; (Geophysical survey); (passed the 180° meridian).
4	bc, c	24.30	351.0	(Geophysical survey).
5	bc, c	24.30	343.8	(Geophysical survey).
6	bc, c	24.30	338.3	(Geophysical survey).
7	bc	24.30	333.2	(Geophysical survey).
8	bc, o, c	24.30	333.5	(Geophysical survey).
9	b, bc, c, o	24.30	341.7	(Geophysical survey).
10	bc, b, o	24.00	293.7	(Geophysical survey).
11	o, c, bc	15.15	189.3	(Geophysical survey); ar. off Chiba (13: 15).
12	r, o	1.00	6.5	Ar. Funabashi.

Total cruising day, 60 days; total cruising time, 49 days 14 h 00 min.; total cruising distance, 12,213.8 n.m. (nautical miles).

*Showing both in Japan date and on-site date in parentheses.

**Each abbreviation stands for as follows; b-blue sky; bc-sky partly clouded; c-generally clouded; o-over cast; r-rain; d-drizzle; q-squall.

***Showing in n.m. (nautical miles).

****(Geophysical survey) showing the survey without continuous seismic profiling, and sampling usually accompanies simultaneous photographing by freefall camera sampler.

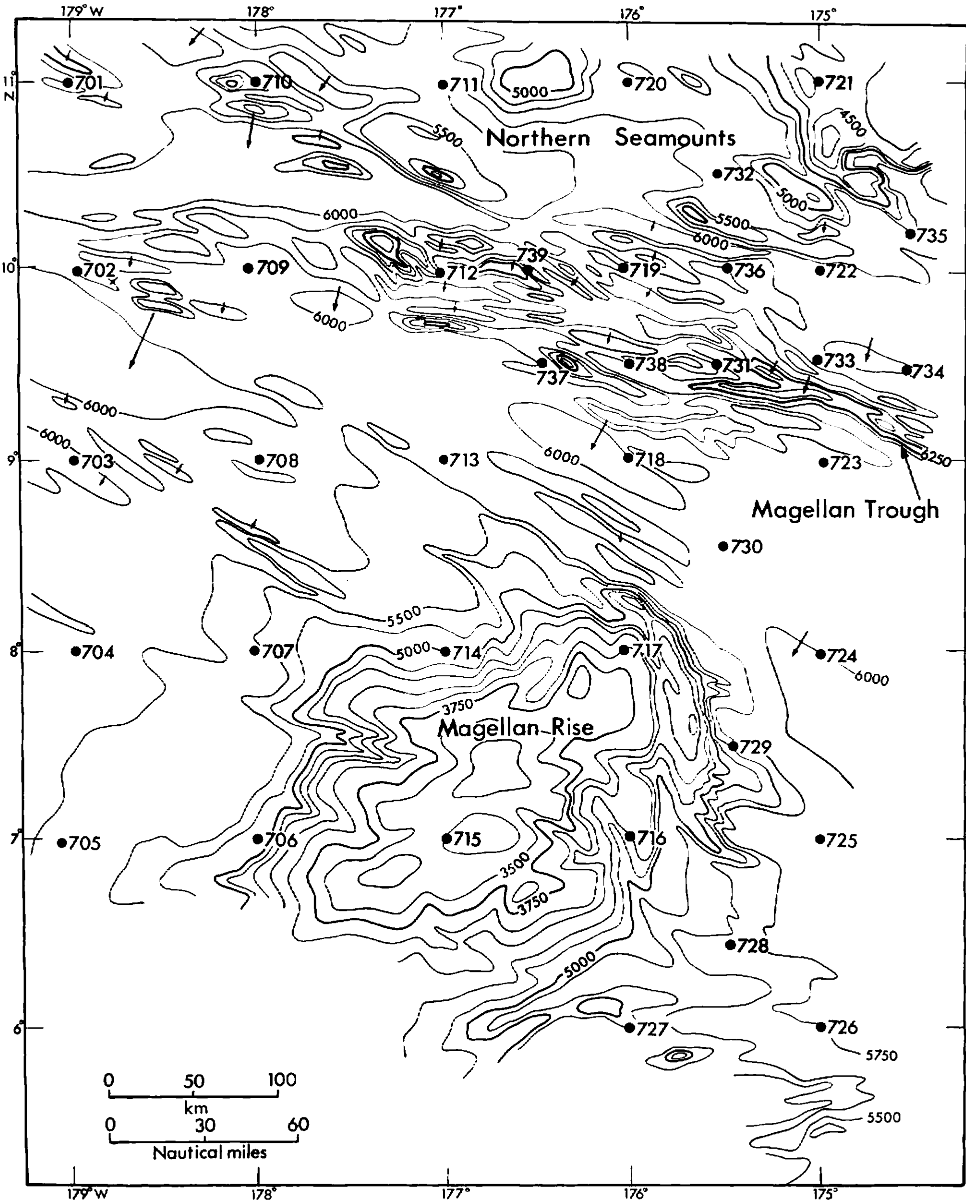

Fig. I-3 Bathymetric map and major stations of on-site observation in GH77-1 area.

tion profiling, proton magnetometer, and on-board gravimeter were carried out regularly between two stations, in the course of ship's shifting from one station to another, throughout nearly the whole area with a ship speed of about 10 knots.

Ship's position was determined by NNSS throughout the survey area. The real time positions obtained were recalculated on the basis of estimated water current to make the accuracy as high as possible. As an improvement in sampling techniques, the check

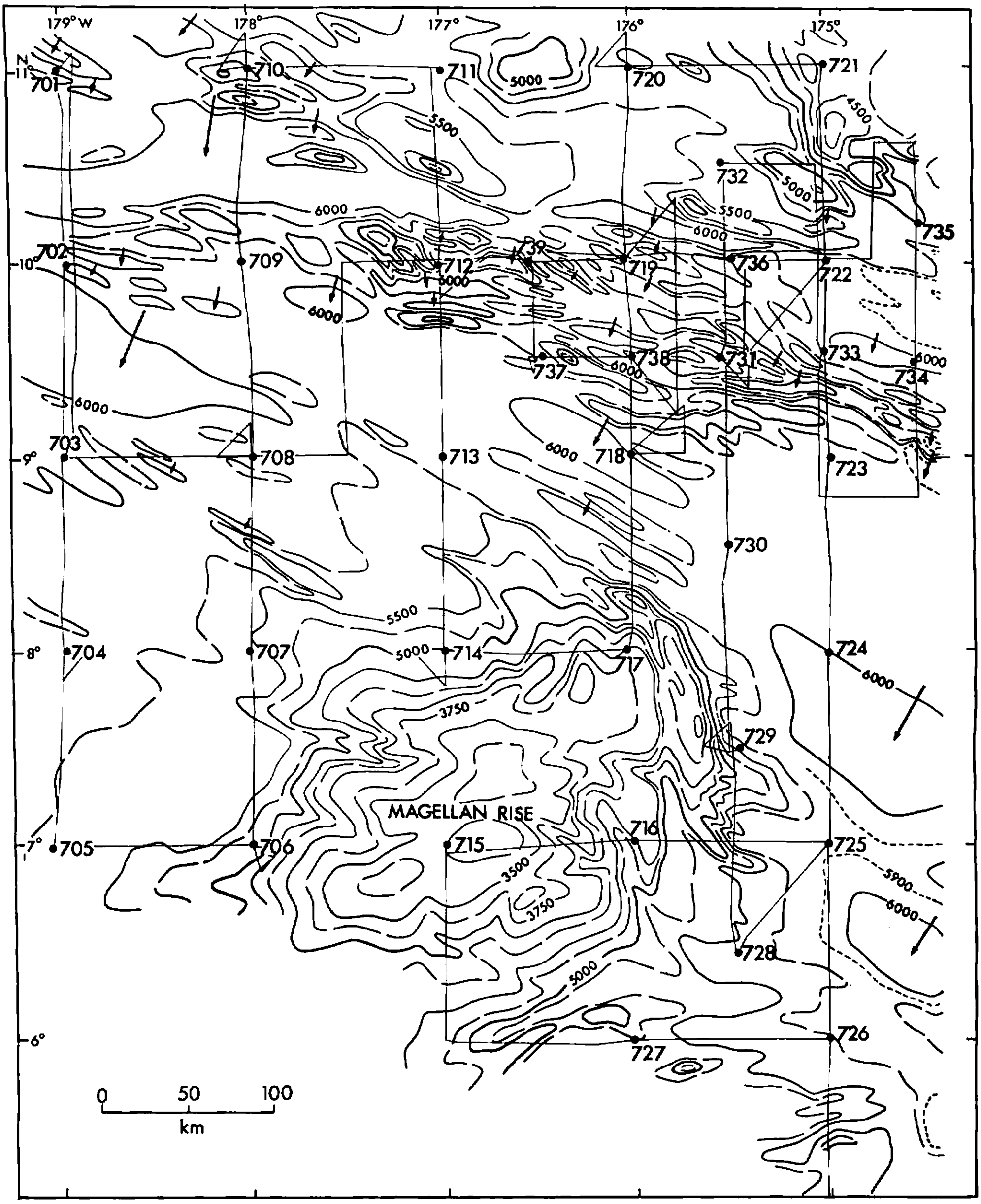

Fig. I–4 Geophysical survey tracks shown on bathymetric map in GH77–1 area.

method of operation of Okean-70 grab at the sea bottom by means of a pinger record was established.

The samples were analyzed also in the on-shore laboratory after the cruise by the GSJ staffs including non-on-board members: the remanent magnetization measurement of piston core samples by M. JOSHIMA; chemical analysis of manganese nodules by T.

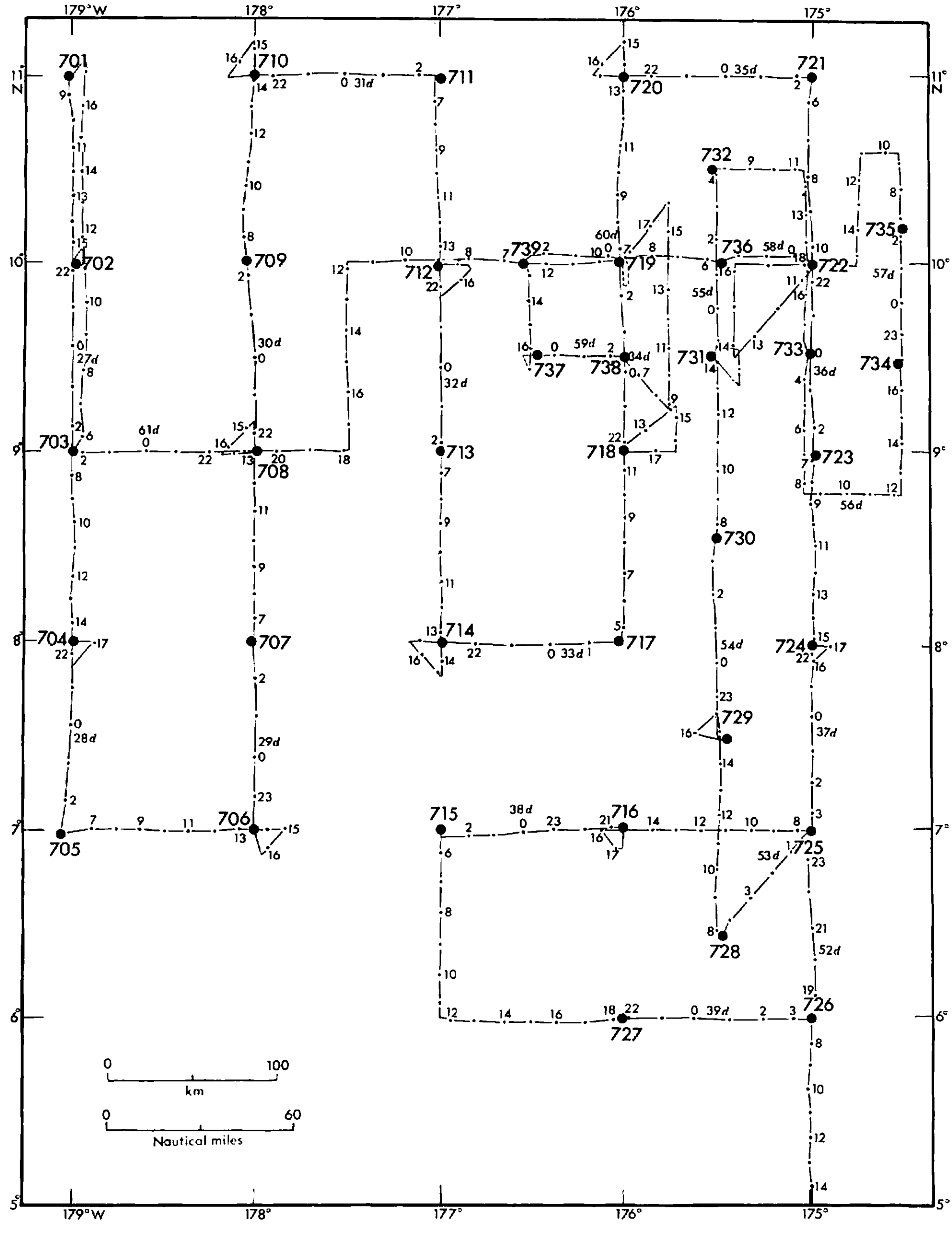

Fig. I–5 Details of stations of on-site observation (solid circles) and geophysical survey tracks (lines with dots showing GMT date and time).

MOCHIZUKI and S. TERASHIMA; chemical analysis of surface sediments by K. KATO.

Summary of investigation results at GH77–1 area

The results of the whole on-site observations are summarized in Table I–5 together

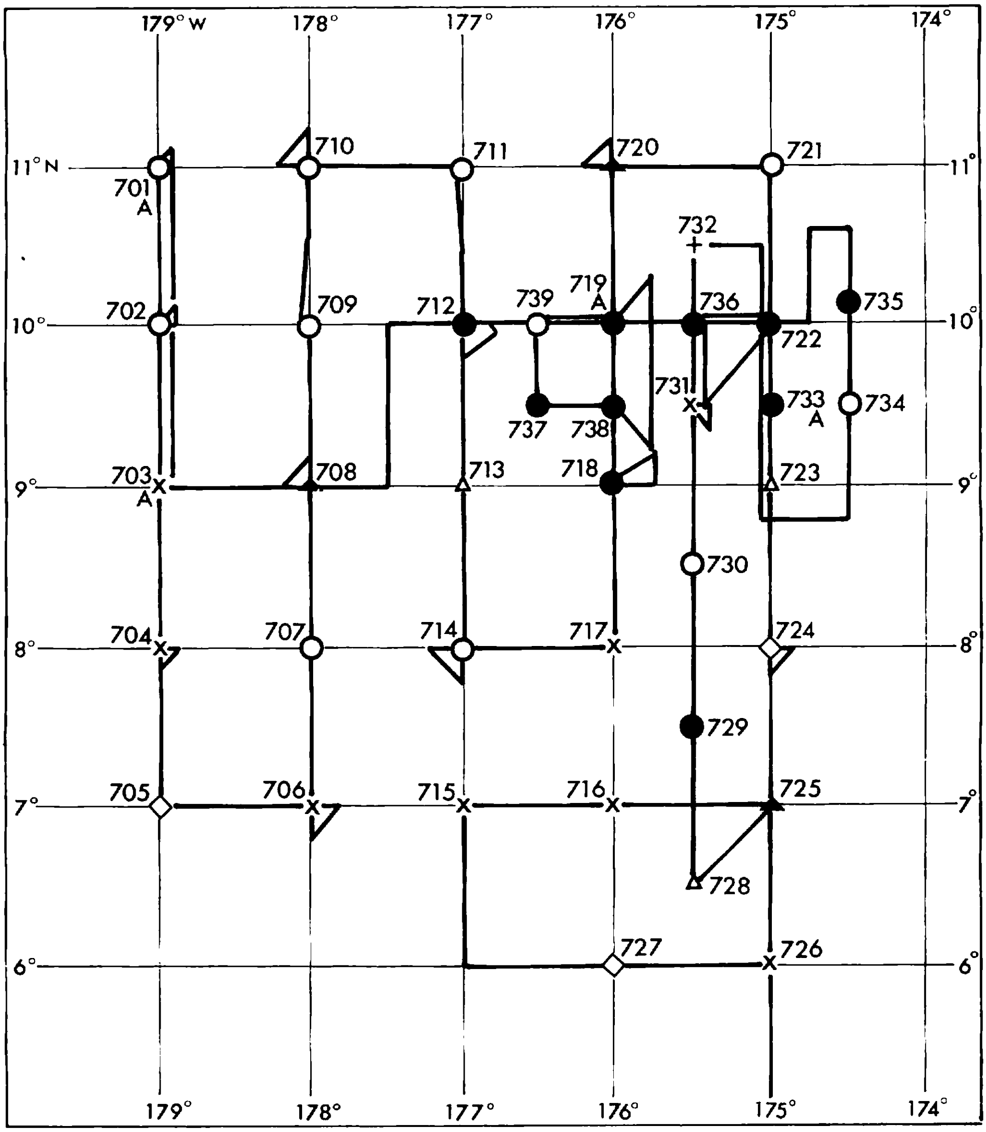

Marks showing degree of nodule abundance in kg/m²

× 0 + <0.1 ◇ 0.1–1.0 △ 1.0–5.0 ▲ 5.0–10.0 ○ 10.0–20.0 ● >20.0

Fig. I–6 Generalized map of survey stations and geophysical survey tracks, with indication of nodule abundance.

with the corrected depth for the velocity of sound in seawater according to MATTHEWS' Table and recalculated position of each station. The recalculated position is considered to have an error, in most cases, either within 0.25–0.55 km under favorable conditions or around 0.9 km under unfavorable conditions.

These results enabled us to understand the characteristics and distribution of the

Table I–5 Results of

St. No.	Observ.[1] No.	Julian Day	Local Day	Local Time ▼[2]	Local Time ▲	Position Lat. (N) ▼	Position Long. (W) ▼	Position Lat. (N) ▲	Position Long. (W) ▲
701	(G372)	026	1.26	18:12		10 59 7	179 02 6		
	FG33–1	〃	〃	16:05		10 59 6	179 01 6		
	〃 C	〃	〃	〃		〃	〃		
	FG33–2	〃	〃	16:09		10 59 7	179 01 4		
	〃 C	〃	〃	〃		〃	〃		
701A	G405	061	3.2	08:53		10 58 0	179 01 6		
702	G373	026	1.26	07:45		09 58 9	178 59 3		
	FG34–1	〃	〃	06:00		09 59 1	178 59 1		
	〃 C	〃	〃	〃		〃	〃		
	FG34–2	〃	〃	06:05		09 59 1	178 58 9		
	〃 C	〃	〃	〃		〃	〃		
703	(G374)	027	1.26	16:58		08 59 2	178 59 3		
	FG35–1	〃	〃	14:52		08 59 3	178 59 3		
	〃 C	〃	〃	〃		〃	〃		
	FG35–2	〃	〃	14:56		08 59 0	178 59 3		
	〃 C	〃	〃	〃		〃	〃		
703A	G404	061	3.1	15:57		08 59 4	179 00 5		
704	G375	027	1.27	08:06		07 57 6	179 00 2		
	FG36–1	〃	〃	06:25		07 58 2	179 00 0		
	〃 C	〃	〃	〃		〃	〃		
	FG36–2	〃	〃	06:28		07 57 9	179 00 0		
	〃 C	〃	〃	〃		〃	〃		
705	G376	028	1.27	16:28		06 58 3	179 02 2		
	FG37–1	〃	〃	14:53		06 58 8	179 01 8		
	〃 C	〃	〃	〃		〃	〃		
	FG37–2	〃	〃	14:56		06 58 5	179 01 8		
	〃 C	〃	〃	〃		〃	〃		
706	G377	028	1.28	07:43		06 59 2	178 00 1		
	FG38–1	〃	〃	06:05		06 59 9	177 59 7		
	(〃 C)	〃	〃	〃		〃	〃		
	FG38–2	〃	〃	06:08		06 59 7	177 59 9		
	〃 C	〃	〃	〃		〃	〃		
707	G378	029	1.28	16:37		08 00 0	178 01 1		
	FG39–1	〃	〃	14:59		07 59 9	178 00 4		
	〃 C	〃	〃	〃		〃	〃		
	FG39–2	〃	〃	15:02		08 00 1	178 00 4		
	〃 C	〃	〃	〃		〃	〃		

on-site observations.

Depth (m)	Mn-nodule abundance[3)]		Results and remarks		
		kg/m²	Bottom materials[4)] [ ] showing results of sediment type analysis		Remarks[5)]. Topography, ( ) showing 3.5 kHz transparent layer
5,940	—	—	—		Top of a small hill in rolled topography.
〃	(△)	(3.8)		Ss/SPs, DPs	
〃		[50%]		Ss/SPs	
〃	○	17.7	[Siliceous clay]		Slope to foot of a small hill in rolled topography.
〃		[50%]			〃
6,000		(7.1)	[Deep sea clay]	Ss/SPs	〃
5,950	▲	9.8	[Deep sea clay]	IDPs, Vs, Phosphorite	Top of a hill in ragged topography.
5,900		—			
〃		[30%]	Slab like large nodules		
〃	○	12.0	[Deep sea clay]	Ss/SPs, IDPs	
〃		[30%]			
5,985	—	—	—		Floor of flat topography with occasional hills.
5,970	×	0	[Deep sea clay]		
〃		[0%]			
5,980	×	0			
〃		[0%]			
5,990	×	0	[Deep sea clay]		
5,860	×	0	[Deep sea clay]		Floor of flat topography.
5,870	×	0	[Deep sea clay]		
〃		[0%]			
〃	×	0			
〃		[0%]			
5,660	◇	0.2	[Siliceous clay]	Sr	Gentle slope of a rolled hill area among flat topography.
5,620	◇	0.3	[Deep sea clay]	Sr, SPr	
〃					
5,640	+	<0.1		Sr	
〃					
5,225	×	0	[Siliceous clay]	Subangular basalt, red chert fragments	Floor of a terrace like plane along western foot of Magellan Rise.
〃	×	0		Basalt, red chert fragments	
〃		—	—		
〃	×	0		Basalt, red chert fragments	
〃	R	⟨40%⟩	Rock fragments		
5,590	△	3.9	[Siliceous clay]	SPr, Vr(slab)	Floor of very gently rolled area along northwestern foot of Magellan Rise.
5,600	○	10.9		SPr	
〃		[30%]	[Deep sea clay]		
5,590	◇	0.2		SPr	
〃		[2%]			

Table I–5

St. No.	Observ.[1] No.	Julian Day	Local Day	Local Time ▼[2]	Local Time ▲	Position Lat. (N) ▼	Position Long. (W) ▼	Position Lat. (N) ▲	Position Long. (W) ▲
708	G379	029	1.29	07:37		08 59 5	177 59 5		
	FG40–1	〃	〃	05:55		08 59 9	177 58 8		
	〃 C	〃	〃	〃		〃	〃		
	FG40–2	〃	〃	05:58		08 59 7	177 59 0		
	〃 C	〃	〃	〃		〃	〃		
709	G380	030	1.29	16:18		10 01 2	178 02 1		
	FG41–1	〃	〃	14:37		10 00 8	178 01 9		
	〃 C	〃	〃	〃		〃	〃		
	FG41–2	〃	〃	14:40		10 01 1	178 01 9		
	〃 C	〃	〃	〃		〃	〃		
710	G381	030	1.30	07:48		10 59 4	178 00 2		
	FG42–1	〃	〃	06:10		11 00 4	177 59 7		
	〃 C	〃	〃	〃		〃	〃		
	FG42–2	〃	〃	06:13		11 00 4	177 59 9		
	〃 C	〃	〃	〃		〃	〃		
711	G382	031	1.30	16:18		10 59 3	176 59 4		
	FG43–1	〃	〃	14:48		10 59 6	176 59 1		
	〃 C	〃	〃	〃		〃	〃		
	FG43–2	〃	〃	14:51		10 59 5	176 58 9		
	〃 C	〃	〃	〃		〃	〃		
712	G383	031	1.31	07:33		09 59 2	177 00 5		
	FG44–1	〃	〃	06:00		09 59 5	177 00 2		
	〃 C	〃	〃	〃		〃	〃		
	FG44–2	〃	〃	06:03		09 59 5	177 00 4		
	〃 C	〃	〃	〃		〃	〃		
713	G384	032	1.31	15:59		08 58 2	177 00 1		
	FG45–1	〃	〃	14:26		08 59 8	177 00 0		
	〃 C	〃	〃	〃		〃	〃		
	FG45–2	〃	〃	14:32		08 59 2	177 00 1		
	〃 C	〃	〃	〃		〃	〃		
714	G385	032	2.1	07:31		07 59 4	176 59 0		
	FG46–1	〃	〃	06:10		07 59 8	176 59 2		
	〃 C	〃	〃	〃		〃	〃		
	FG46–2	〃	〃	06:13		07 59 8	176 59 0		
	〃 C	〃	〃	〃		〃	〃		

(Continued)

Depth (m)	Mn-nodule abundance[3]	kg/m²	Results and remarks: Bottom materials[4] [ ] showing results of sediment type analysis		Remarks[5]. Topography, ( ) showing 3.5 kHz transparent layer
5,760	▲	8.4	[Deep sea clay]	SPr, Sr	Top of a small hill in rolled topography.
5,795	△	2.9	[Siliceous clay]	SPr, Sr	
〃		[3%]			
5,805	△	2.2		SPr, Sr	
〃		[3%]			
5,850	○	16.5	[Deep sea clay]	DPs, IDPs	Top of a small hill of repeated hills and troughs topography.
5,860	(◇)	(0.5)		DPs	
〃		[60%]			
5,860	(△)	(2.8)		DPs	
〃		[60%]			
5,550	○	17.4	[Deep sea clay]	DPs, Ss/SPs, IDPs	Steep slope of a hill in ragged topography.
〃	○	11.4	[Deep sea clay]	DPs, Ss/SPs, IDPs	
〃		[65%]			
5,650	△	2.5		DPs, Ss/SPs, IDPs	
〃		[8%]			
5,740	×	0	[Calcareous-siliceous clay]		Bottom of an inter-hill small basin along western foot of a seamount.
〃	○	15.4		Ss/SPs, DPs	
〃		[75%]			
〃	◇	0.2	[Siliceous clay]	Slaty chert frag., Ss/SPs, DPs	
〃	R	〈70%〉	Rock fragments		
5,915	●	21.1	[Deep sea clay]	DPs, Ss/SPs, IDPs	Floor of a small flat basin in repeated hills and troughs topography.
5,900	○	11.3		Ss/SPs, DPs, IDPs	
〃		[50%]			
〃	(△)	(1.9)	[Siliceous clay]	DPs, IDPs	
〃		[55%]			
5,920	△	3.4	[Deep sea clay]	Sr, SPr	Floor of southern margin of nearly flat extensive basin.
5,940	△	2.9	[Deep sea clay]	Sr, SPr	
〃		[5%]			
5,920	◇	0.5		Sr, SPr	
〃		[5%]			
5,120	○	14.8	[Siliceous clay]	Ss/SPs, DPs, IDPs	Slope of gently rolled northern lower slope to foot of Magellan Rise.
5,070	▲	9.7		Ss/SPs, DPs, IDPs	
〃		[40%]			
5,090	(△)	(1.4)		Ss/SPs, DPs	
〃		[35%]			

Table I-5

St. No.	Observ.[1] No.	Julian Day	Local Day	Local Time ▼[2]	Local Time ▲	Position Lat. (N) ▼	Position Long. (W) ▼	Position Lat. (N) ▲	Position Long. (W) ▲
715	G396	038	2.6	15:58		06 57 9	177 00 9		
	FG57–1	〃	〃	15:03		06 58 2	177 00 5		
	〃 C	〃	〃	〃		〃	〃		
	FG57–2	〃	〃	15:06		06 58 2	177 00 7		
	〃 C	〃	〃	〃		〃	〃		
716	G396	037	2.6	07:30		07 01 4	176 00 1		
	FG56–1	〃	〃	06:14		07 01 2	176 00 1		
	〃 C	〃	〃	〃		〃	〃		
	FG56–2	〃	〃	06:17		07 01 5	176 00 1		
	〃 C	〃	〃	〃		〃	〃		
717	G386	033	2.1	15:09		08 00 0	176 00 1		
	FG47–1	〃	〃	14:00		08 00 3	176 00 1		
	〃 C	〃	〃	〃		〃	〃		
	FG47–2	〃	〃	14:03		08 00 4	176 00 0		
	〃 C	〃	〃	〃		〃	〃		
718	G387	033	2.2	07:52		08 59 0	176 01 7		
	FG48–1	〃	〃	06:10		08 59 5	176 01 0		
	〃 C	〃	〃	〃		〃	〃		
	FG48–2	〃	〃	06:13		08 59 5	176 01 2		
	〃 C	〃	〃	〃		〃	〃		
719	G388	034	2.2	16:36		10 00 0	176 01 4		
	FG49–1	〃	〃	15:06		10 00 8	176 01 2		
	〃 C	〃	〃	〃		〃	〃		
	FG49–2	〃	〃	15:10		10 00 8	176 01 3		
	〃 C	〃	〃	〃		〃	〃		
719A	FG71–1	059	2.28	06:38		09 58 1	176 00 4		
	FG71–2	〃	〃	06:55		09 56 2	176 00 5		
	〃 C	〃	〃	〃		〃	〃		
	FG71–3	〃	〃	07:10		09 54 4	176 00 6		
	FG71–4	〃	〃	07:24		09 52 5	176 00 8		
	〃 C	〃	〃	〃		〃	〃		
	FG71–5	〃	〃	07:44		09 53 8	175 58 9		
	FG71–6	〃	〃	08:00		09 55 9	175 59 1		
	FG71–7	〃	〃	08:16		09 57 9	175 59 2		
	〃 C	〃	〃	〃		〃	〃		
	FG71–8	〃	〃	08:32		10 00 0	175 59 3		

(Continued)

Depth (m)	Mn-nodule abundance[3]		Results and remarks		
		kg/m²	Bottom materials[4) [ ] showing results of sediment type analysis		Remarks[5). Topography, ( ) showing 3.5 kHz transparent layer
3,250	×	0	[Calcareous ooze]		Top of a hill on fairly ragged topography of the top of Magellan Rise.
3,240	×	0	[Calcareous ooze]		
〃		[0%]			
〃	×	0			
〃		[0%]			
4,254	×	0	[Calcareous ooze]		Top of a large hill or spur on fairly ragged eastern slope of Magellan Rise.
4,244	×	0	[Calcareous ooze]		
〃		[0%]			
〃	×	0			
〃		[0%]			
3,997	×	0	[Calcareous ooze]		Top of a small hilly part in fairly ragged topography along northeastern slope of Magellan Rise.
4,018	×	0	[Calcareous clay]		
〃		[0%]			
〃	×	0			
〃		[0%]			
6,035	○	18.9	[Deep sea clay]	Ss/SPs, DPs	Bottom of a hill or margin of a basin in repeated hills and troughs topography.
6,014	○	17.5	[Siliceous clay]	DPs, Ss/SPs	
〃		[60%]			
〃	●	20.5		DPs, Ss/SPs, IDPs	
〃		[60%]			
5,500	●	23.7	[Deep sea clay]	DPs, ISs, IDPs, Vs(n.f.)	A series of parts along a hill top to a trough bottom in hills and troughs topography.
5,556	●	26.6	[Siliceous clay]	DPs/ISs, Vs(n.f.)	G388・FG49-1・49-2:
〃		[75%]			Upper slops of hill
5,566	○	(16.9)		DPs, IDPs, ISs, Vs(n.f.)	FG71−1: Top of hill, TL (15 m)
〃		[75%]			−2: Bottom of hill, 〃 (10 m) −3: Floor of trough, 〃 (1 m)
5,464	●	25.9		ISs, IDPs, Vs(n.f.)	−4: 〃 , 〃 (5 m)
5,785	●	23.5	[Deep sea clay]	ISs, IDPs, Vs(n.f.)	−5: 〃 , 〃 (5 m)
〃		[65%]			−6: Bottom of hill, 〃 (0 m)
5,828	○	17.4		DPs, IDPs	−7: Top of hill, 〃 (15 m)
5,815	●	23.6	[Deep sea clay]	DPs, Ss/SPs, IDPs	−8: A valley head on upper slope of hill, 〃 (20 m)
〃		[70%]			
5,858	○	16.4		DPs, ISs, IDPs	
5,848	○	18.1		DPs, ISs, IDPs, Vs(n.f.)	
5,484	●	26.1	[Siliceous clay]	DPs, IDPs, ISs, Vs(n.f.)	
〃		[70%]			
5,598	●	27.6		ISs, IDPs, Vs(n.f.)	

Table I-5

St. No.	Observ.[1)] No.	Julian Day	Local Day	Local Time ▼[2)]	Local Time ▲	Position Lat. (N) ▼	Position Long. (W) ▼	Position Lat. (N) ▲	Position Long. (W) ▲
720	G389	034	2.3	07:42		10 59 2	175 59 0		
	FG50–1	〃	〃	06:12		10 59 5	175 59 2		
	〃 C	〃	〃	〃		〃	〃		
	FG50–2	〃	〃	06:15		10 59 4	175 58 9		
	〃 C	〃	〃	〃		〃	〃		
721	G390	035	2.3	15:51		10 59 6	174 59 9		
	FG51–1	〃	〃	14:33		10 59 5	174 59 5		
	〃 C	〃	〃	〃		〃	〃		
	FG51–2	〃	〃	14:35		10 59 5	174 59 3		
	〃 C	〃	〃	〃		〃	〃		
722	G391	035	2.4	07:52		09 59 8	174 59 9		
	FG52–1	〃	〃	06:17		09 59 9	174 59 3		
	〃 C	〃	〃	〃		〃	〃		
	FG52–2	〃	〃	06:20		10 00 0	174 59 3		
	〃 C	〃	〃	〃		〃	〃		
722A	D212	057	2.26	08:18	09:11	09 59 1	175 02 1	09 59 1	175 03 8
723	G392	036	2.4	16:24		08 57 8	174 59 4		
	FG53–1	〃	〃	14:41		08 59 1	174 59 1		
	〃 C	〃	〃	〃		〃	〃		
	FG53–2	〃	〃	14:47		08 58 9	174 59 0		
	〃 C	〃	〃	〃		〃	〃		
724	G393	036	2.5	07:52		08 00 0	175 00 6		
	FG54–1	〃	〃	06:15		08 00 0	175 00 3		
	〃 C	〃	〃	〃		〃	〃		
	FG54–2	〃	〃	06:17		08 00 0	175 00 5		
	〃 C	〃	〃	〃		〃	〃		
725	G394	037	2.5	17:23		06 57 7	175 00 4		
	FG55–1	〃	〃	15:49		06 58 0	174 59 9		
	〃 C	〃	〃	〃		〃	〃		
	FG55–2	〃	〃	15:53		06 57 7	174 59 9		
	〃 C	〃	〃	〃		〃	〃		
726	G398	039	2.7	17:13		06 00 4	174 59 5		
	FG59–1	〃	〃	15:40		06 00 4	174 59 6		
	〃 C	〃	〃	〃		〃	〃		
	FG59–2	〃	〃	15:42		06 00 5	174 59 4		
	〃 C	〃	〃	〃		〃	〃		

(Continued)

Depth (m)	Mn-nodule abundance[3]	kg/m²	Bottom materials[4] [ ] showing results of sediment type analysis		Results and remarks: Remarks[5]. Topography, ( ) showing 3.5 kHz transparent layer
5,536	△	3.6	[Siliceous clay]	Ss/SPs	Top of a small hill in very gently rolled topography.
5,346	▲	6.5		Ss/SPs	
〃		[20%]			
5,565	△	4.0	[Deep sea clay]	Ss/SPs	
〃		[20%]			
4,580	○	16.4	[Calcareous-siliceous clay]	DPs, Vs(n.f.)	Flat top of a seamount with 1000 m height.
〃	(▲)	(7.4)	[Calcareous-siliceous clay]	DPs, Vs(n.f.)	
〃		[65%]			
4,590	(△)	(4.7)		DPs, Vs(n.f.)	
〃		[65%]			
4,796	○	19.9	[Siliceous clay]	IDPs, DPs, Vs(n.f.)	Flat floor at northern marginal part of "northern nodule abundant area" of gently rolled to flat topography.
〃	●	28.1		IDPs, DPs, Vs(n.f.)	
〃		[70%]			
〃	●	23.5	[Deep sea clay]	IDPs, DPs, Vs(n.f.)	
〃		[70%]			
5,806 –5,821	Total weight	(180 kg)		IDPs, DPs, Vs(n.f.)	
5,952	△	1.0	[Deep sea clay]	Sr, SEr	Floor of flat topography just south of "Magellan Trough".
〃	△	1.4		Sr	
〃		[5%]			
〃	△	2.5	[Deep sea clay]	Sr, SPr	
〃		[10%]			
5,950	◇	0.5	[Deep sea clay]	Sr, SPr	Floor of extensively flat topography with a gently rolled part near the site.
〃	◇	0.6		Sr, SPr	
〃		[0%]			
〃	◇	0.5	[Deep sea clay]	Sr, SPr	
〃		[0%]			
5,940	▲	7.7	[Deep sea clay]	Sr, Db, Vr(slab)	Floor of extensively flat topography.
〃	+	<0.1		SPr	
〃		[0%]			
〃	+	<0.1	[Deep sea clay]	Sr, SPr	
〃		[0%]			
5,723	×	0	[Siliceous clay]		Floor of extensively flat topography.
〃	×	0			
〃		[0%]			
〃	×	0			
〃		[0%]			

Table I-5

St. No.	Observ.[1] No.	Julian Day	Local Day	Time ▼[2]	Time ▲	Position Lat. (N) ▼	Position Long. (W) ▼	Position Lat. (N) ▲	Position Long. (W) ▲
727	G397	038	2.7	08:11		05 59 1	176 01 5		
	FG58-1	〃	〃	06:43		05 59 9	176 00 5		
	〃 C	〃	〃	〃		〃	〃		
	FG58-2	〃	〃	06:46		05 59 8	176 00 9		
	〃 C	〃	〃	〃		〃	〃		
728	P97	053	2.21	18:01		06 29 2	175 28 5		
	FG60-1	〃	〃	16:32		06 29 2	175 28 3		
	〃 C	〃	〃	〃		〃	〃		
	FG60-2	〃	〃	16:39		06 29 8	175 28 3		
	(〃 C)	〃	〃	〃		〃	〃		
729	P98	053	2.22	07:50		07 29 3	175 26 5		
	FG61-1	〃	〃	06:20		07 29 8	175 26 3		
	〃 C	〃	〃	〃		〃	〃		
	FG61-2	〃	〃	06:24		07 29 8	175 26 0		
	〃 C	〃	〃	〃		〃	〃		
730	P99	054	2.22	17:13		08 32 8	175 30 2		
	FG62-1	〃	〃	15:46		08 32 6	175 30 0		
	〃 C	〃	〃	〃		〃	〃		
	FG62-2	〃	〃	15:49		08 32 8	175 29 9		
	〃 C	〃	〃	〃		〃	〃		
731	P100	054	2.23	07:44		09 30 0	175 32 2		
	(FG63-1)	〃	〃	06:12		09 30 3	175 32 0		
	(〃 C)	〃	〃	〃		〃	〃		
	FG63-2	〃	〃	06:15		09 30 3	175 32 3		
	〃 C	〃	〃	〃		〃	〃		
732	P101	055	2.23	17:35		10 30 7	175 30 5		
	FG64-1	〃	〃	16:11		10 30 7	175 29 9		
	〃 C	〃	〃	〃		〃	〃		
	FG64-2	〃	〃	16:15		10 31 0	175 29 8		
	〃 C	〃	〃	〃		〃	〃		
733	(G(B)399)	055	2.24	08:15		09 29 3	174 59 7		
	FG65-1	〃	〃	06:24		09 29 8	174 59 4		
	〃 C	〃	〃	〃		〃	〃		
	FG65-2	〃	〃	06:27		09 29 9	174 59 3		
	〃 C	〃	〃	〃		〃	〃		

(Continued)

Depth (m)	Results and remarks				
	Mn-nodule abundance[3) kg/m²]		Bottom materials[4)] [ ] showing results of sediment type analysis		Remarks[5)]. Topography, ( ) showing 3.5 kHz transparent layer
5,371	◇	0.6	[Deep sea clay]	Sr	Bottom of a hill in flat topography along southeastern foot of Magellan Rise.
5,380	×	0			
〃		[0%]			
〃	×	0			
〃		[0%]			
5,560			[Deep sea clay]		Floor of nearly flat topography surrounded by small hills at south-eastern foot of Magellan Rise.
5,535	◇	0.6		Sr	
〃		[0%]			
5,556	△	1.2	[Deep sea clay]	Sr	
〃		—			
5,795			[Deep sea clay]		Floor of nearly flat topography at eastern foot of Magellan Rise.
〃	●	25.5		Ss/SPs, IDPs	
〃		[55%]			
〃	○	19.3		Ss/SPs	
〃		[55%]			
5,865			[Deep sea clay]		Slope to bottom floor of a low hill in gently rolled topography.
〃	○	11.5		SPr, Sr	
〃		—			
〃	▲	9.7		SPr, Sr	
〃		[25%]			
6,136			[Siliceous ooze]		Floor of a graben like plane in hills and troughs topography.
〃		—			
〃		—			
〃	×	0			
〃		[0%]			
5,690			[Siliceous ooze]		Floor of fairly extensive plain.
5,680	+	<0.1		Sr	
〃		[0%]			
〃	+	<0.1	[Siliceous ooze]	Sr	
〃		[0%]			
5,920		—	—		Floor of a terrace like low hill at marginal part of "northen nodule abundant area," just north of a horst like wall ridge of "Magellan Trough".
〃	●	21.7	[Siliceous clay]	ISs, DPs, IDPs, Vs(n.f.)	
〃		—			
〃	●	24.2		ISs, DPs, IDPs, Vs(n.f.)	
〃		[65%]			

Table I–5

St. No.	Observ.[1] No.	Julian Day	Local			Position			
			Day	Time		Lat. (N)	Long. (W)	Lat. (N)	Long. (W)
				▼[2]	▲	▼	▼	▲	▲
733A	D211	055–056	2.24	12:13	13:00	09 30 5	175 02 6	09 30 6	175 03 2
734	(G(B)400)	056	2.25	08:29		09 28 0	174 30 4		
	FG66–1	〃	〃	06:10		09 29 2	174 29 9		
	〃 C	〃	〃	〃		〃	〃		
	FG66–2	〃	〃	06:14		09 29 0	174 30 2		
	(〃 C)	〃	〃	〃		〃	〃		
735	C11	057	2.25	16:00	16:50	10 10 5	174 30 5		
	FG67–1	〃	〃	14:14		10 10 2	174 30 5		
	〃 C	〃	〃	〃		〃	〃		
	FG67–2	〃	〃	14:17		10 10 4	174 30 5		
	〃 C	〃	〃	〃		〃	〃		
736	(G(B′)401)	058	2.26	16:13		09 59 1	175 29 8		
	FG68–1	〃	〃	14:40		09 59 4	175 29 2		
	〃 C	〃	〃	〃		〃	〃		
	FG68–2	〃	〃	14:43		09 59 3	175 29 5		
	〃 C	〃	〃	〃		〃	〃		
737	C12	058	2.27	08:30	08:59	09 30 4	176 27 4	09 30 3	176 27 6
	FG69–1	〃	〃	06:19		09 30 3	176 27 4		
	〃 C	〃	〃	〃		〃	〃		
	FG69–2	〃	〃	06:22		09 30 4	176 27 2		
	〃 C	〃	〃	〃		〃	〃		
738	G402	059	2.27	16:16		09 29 8	175 58 1		
	FG70–1	〃	〃	14:37		09 30 2	175 58 8		
	〃 C	〃	〃	〃		〃	〃		
	FG70–2	〃	〃	14:39		09 30 2	175 58 5		
	〃 C	〃	〃	〃		〃	〃		
739	G403	060	2.28	16:24		10 00 1	176 32 1		
	FG72–1	〃	〃	14:45		10 00 3	176 31 7		
	〃 C	〃	〃	〃		〃	〃		
	FG72–2	〃	〃	14:49		10 00 1	176 31 9		
	〃 C	〃	〃	〃		〃	〃		

1: G, Okean-70 grab; G(B), Box corer; D, Large box dredge; FG, Freefall photo grab (sample); FG-C, Freefall
2: ▼, on bottom; ▲, roll up start.
3: Abundance is shown in kg/m^2; Marks show abundance grade, × 0, + <0.1, ◇, 0.1–1.0, △, 1.0–5.0, ▲, fect sampling; Parentheses [ ] show cover ratio by a sea bottom photograph.
4: Sediment types are determined principally on the samples by Okean-70 grab (G) and those determined on nodules, shown in the type symbols (See Chap. XIII, in this report).
5: Topographic description is mainly made on the observation of features of 3.5 kHz PDR profiling record

(Continued)

Depth (m)	Results and remarks				
	Mn-nodule abundance[3]		Bottom materials[4] [ ] showing results of sediment type analysis		Remarks[5]. Topography, ( ) showing 3.5 kHz transparent layer
		kg/m²			
5,932 -5,775	Total weight	(300 kg)	Large amount of nodules		
6,035		—	—		Floor of flat plane in central part of "Northern manganise abundant area".
″	○	10.9		Sr, SEr, SPr	
″		[30%]			
″	▲	5.8	[Deep sea clay]	Sr, SPr, SEr	
″		—			
5,484 -5,556		[75%]			Floor of a terrace like plane in gently rolled topography at marginal part of "northern nodule abundant area".
5,495	●	27.7		ISs, DPs, Vs(n.f.)	
″		[75%]			
5,484	○	(11.9)		ISs, DPs, Vs(n.f.)	
″		[75%]			
5,464		—	—		Top of very gentle hill in gently rolled topography.
″	●	27.4		DPs, Ss/SPs	
″		[70%]			
″	●	26.5	[Deep sea clay]	DPs, Ss/SPs	
″		[70%]			
5,743		[70%]			Floor of nearly flat plane between hills in fairly ragged topography.
″	●	23.6		ISs, DPs, Vs(n.f.)	
″		[70%]			
″	●	26.1		ISs, DPs, Vs(n.f.)	
″		[70%]			
6,160	○	14.0	[Deep sea clay]	ISs, DPs, Vs(n.f.)	Floor of a deep trough in hills and troughs topography.
6,140	○	14.6		ISs, DPs, IDPs	
″		[65%]			
6,150	●	26.2	[Deep sea clay]	ISs, IDPs, DPs	
″		[65%]			
5,951		—	[Deep sea clay]	Ss/SPs	Slope of a hill in ragged topography.
5,931	○	18.6		DPs, Ss/SPs	
″		[70%]			
5,869	○	16.4		IDPs, DPs, ISs	
″		[70%]			

photo grab (photograph); P, Corer; C, Deep sea camera.

5.0–10.0, ○, 10.0–20.0, ●, $>$ 20.0 kg/m²; Parentheses ( ) indicate uncertain value probably due to imper-

small quantity of freefall grab sample (FG) are very questionable and shown only for reference; Manganese

on site survey.

manganese nodule deposit, and its relationship to submarine topography, bottom sediments, acoustic stratigraphy and structure of the substrate layers. Also, some of these data gave an important information for the reconstruction of the geologic development of Central Pacific Basin. In addition, some preliminary data on the movement of sea-water mass were obtained. These are summarized as below.

GH77–1 area is topographically divided largely into two topographic plateau like highs of the southern Magellan Rise at a depth of 3,250 m and the northern seamounts at a depth of 4,250 m, and remaining deep sea basin characterized by the developments either of the repeated linear hills and troughs of WNW trend or abyssal plain. The deep sea basin area is subdivided into the raised broad zone with marked topographic relief trending in NNE direction from the Magellan Rize, the eastern and western deep sea basins located either sides of the raised NNE zone, and the Magellan Trough at a depth deeper than 6,500 m running in WNW direction along the northern margin of the eastern basin area. However, the Magellan Trough extending from the neighboring GH76–1 area branches and loses its clear linearment, around the above-said NNE trend raised zone.

These topographic features closely relate to the acoustic substrate stratigraphy or crustal features by the geophysical survey data, distribution of surface sediments, and distribution of manganese nodules.

The fan-shaped lineation stripe pattern of magnetic anomaly (Magellan lineation), which was found in the GH76–1 area and interpreted as having relation to the formation of oceanic basaltic crust along the Magellan Trough as the spreading center in the Cretaceous age (TAMAKI *et al.*, in press), was recognized in the present GH77–1 area. However, the lineation pattern divides and becomes obscure around the place where the trough crosses the NNE trending raised zone, showing a clear coincidence with topography. Distribution of free air gravity anomaly shows highest value of 15 milligal at topographic highs as the Magellan Rise, lowest values of −35 milligal at the trough reflecting the effect of topography and lower values of −30 milligal over the southeastern deep sea basin area presumably representing the effect of thick sediment accumulation.

Features of the acoustic stratigraphy and structure of the substrate differ in each topographic areas, as Magellan Rise, the remaining deep sea basins and Magellan Trough. In the deep sea basins, the acoustic sequence is divided in descending order into Unit I layer (Type A and Type C), Unit II layer, and the acoustic basement. Type A layer which is acoustically transparent and presumed as oozy and clayey sediments of Neogene to Quaternary, has a thickness of 10–200 m, thickening from north to south. On the other hand, Type C layer, which has a characteristic feature of acoustically stratified turbidites, is developed over the westward and southeastward deep sea basins and forms flat topographic surface of abyssal plain. Unit II layer is acoustically semi-opaque and ranges in thickness from 40 to 250 m, with a reflector said as Middle Eocene–Oligocene chert at its top. The acoustic basement is thought as Cretaceous basalt and constitutes an irregular surface under the Unit I or Unit II layers. At the Magellan Rise area, four acoustic layers are distinguished above its basement, and according to the DSDP data these are a thick accumulation reaching even 1,000 m of limestone, chert, chalk and ooze of Cretaceous to Quaternary age. Magellan Trough is a linear trough bounded by two ridges along its northern and southern walls.

The distribution of surface sediments shows a broad zonal trend that calcareous ooze or calcareous-siliceous clay is confined to the topographic highs as Magellan Rise and the northern seamounts, and these are replaced outwards to deep sea basin successively by siliceous clay, and then by deep sea clay. The siliceous clay is usually of 10 cm thick and underlain by the deep sea clay. Besides, thick siliceous ooze is distributed locally along the boundary between the siliceous clay and deep sea clay areas. Chemical analysis of these surface sediments shows consistent values as the pelagic sediments.

The morphological types of manganese nodules in the present GH77–1 area were revealed to be similar to those of GH76–1 area as a whole. Namely, classification schema of nodules into Sr, SPr, SEr, Db, Ss/SPs, DPs, ISs, IDPs, and V based on the surface structure and shape was applicable to the nodules of this area. However, some slight differences in nodule types exist between the two areas. Of the two fundamental type groups on surface structures, r (rough) and s (smooth) types, the s type group especially of relatively large size seems to be predominant over the r type group in GH77–1 area as compared with the case in GH76–1 area. This tendency is reflected on the chemical composition of manganese nodules, which is characterized by relatively lower contents of the mutually relating Mn, Ni and Cu in GH77–1 area.

Distribution of nodule abundance has relation mainly to topography and the feature of development of acoustic or sedimentary layers, and then, to some extent, to surface sediment types. There exist two contrasting areas, one with high nodule abundance more than 20 kg/m^2 trending in E–W direction in the northern deep sea basin just to the south of the northern seamounts, and the other with almost zero abundance extending southwards along the Magellan Rise and the southeastern deep sea basin. The remaining areas show gradation from the above-said high abundance area to the barren area. The trend is demonstrated also by the data of sea bottom photography on nodule cover ratio.

The northern high nodule abundance area is characterized by the thinner Type A (acoustic transparent) layer of Unit I less than 50 m thick, and by the predominance of deep sea clay rich in radiolarian remains in many cases. On the other hand, the southern barren area is either the place of surface sediments of thick calcareous ooze on the Magellan Rise, or the places represented by thicker Type A layer and Type C layer constituting flat abyssal plain, in both western and southeastern deep sea basins. Another barren area is recognized spottedly in a limited siliceous ooze zone, intruding the northern high abundance area and showing negative relation between nodule distribution and siliceous ooze. However, the surface sediments in the areas with nodule abundance of an order of 10 kg/m^2 are variable, ranging from siliceous-calcareous clay to deep sea clay with lesser amount of radiolarian remains, and they do not necessarily show any relation between manganese nodules and particular sediment types.

From all these facts, it is likely that the distribution of manganese nodules is closely connected with sedimentation history as a whole, and then manganese nodules are confined to such places as having been subjected to less diluting effect on nodule formation by the sediments, or as non-sedimentation since around Oligocene time. Thus, a chronological study of manganese nodules and sediments seems to be very necessary in solving the problem of nodule formation, though we have not any definite data at present. Also, the possibility of contribution of local supply of metal elements of any forms should be investigated, because in spite of similar overall condition of nodule formation there still exist some local variations in nodule abundance and types in some cases. In addition, the data of deep sea photography show many evidences of the activity of benthonic organisms, the role of which presumably should not be negligible on the development of nodules. As another very important point, there is recognized an inverse correlation between the nodule abundance and the grade of Ni and Cu of economical importance (MIZUNO and MORITANI, 1978), and it must be taken into account in resource evaluation of manganese nodule deposits.

References

LARSON, R. L., SMITH, S. M., and CHASE, C. G. (1972) Magnetic lineation of early Cretaceous age in the western equatorial Pacific Ocean. *Earth Planet. Sci. Lett.*, vol. 15, p. 315–319.

MIZUNO, A. and CHUJO, J. (*eds.*) (1975) Deep sea mineral resources investigation in the eastern Central Pacific Basin, August–October 1974 (GH74–5 cruise). *Geol. Surv. Japan Cruise Rept.*, no. 4, 103p.

————. and MORITANI, T. (*eds.*) (1977) Deep sea mineral resources investigation in the central-eastern part of Central Pacific Basin, January–March 1976. *Geol. Surv. Japan Cruise Rept.*, no. 8, 217p.

———— and ———— (1978) Manganese nodule deposits of the Central Pacific. *Preprints 5th Int. Ocean Development Conference* (Tokyo, Sep. 25–29, 1978), B-2, p. 27–39.

TAMAKI, K., JOSHIMA, M., and LARSON, R. L. (1979) Remanent Early Cretaceous spreading center in the Central Pacific Basin. *J. Geophys. Res.* (in press).

WINTERER, E. L., EWING, J. I. *et al.* (1973) *Initial Reports of the Deep Sea Drilling Project*, vol. 17, Washington (U.S. Government Printing Office), xx + 930p.